Low frequency sawtooth precursor in ASDEX Upgrade

G. Papp 1,2), G. I. Pokol 1), G. Por 1), A. Magyarkuti 1), N. Lazányi 1), L. Horváth 1), V. Igochine 3), M. Maraschek 3) and ASDEX Upgrade Team 3)

1) Department of Nuclear Techniques, Budapest University of Technology and Economics, Association EURATOM, Pf 91, H-1521 Budapest, Hungary
2) Department of Applied Physics, Nuclear Engineering, Chalmers University of Technology and Euratom-VR Association, SE-41296 Göteborg, Sweden
3) Max-Planck-Institut für Plasmaphysik, Association EURATOM, D-85748 Garching, Germany

e-mail contact of main author: papp@reak.bme.hu

Abstract. The present paper describes the precursor activity observed in the ASDEX Upgrade tokamak before pronounced sawtooth crashes in various neutral beam heated plasmas, utilizing the soft X-ray diagnostic. Besides the well-known (m, n) = (1, 1) internal kink mode and its harmonics, a Low Frequency Sawtooth Precursor (LFSP) mode is studied in detail. Indications of a second, lower frequency sawtooth precursor have been reported on JET and HT-7 as well. Throughout the studied sawtooth crashes, the power of the lower frequency mode rose by several orders of magnitude just before the crash with a growth rate of 400 1/s, which is shown to be consistent with the growth rate of a resistive core mode. Besides its temporal behaviour, its spatial structure was estimated with a wavelet based method used on SXR measurements, and the most likely value was found to be (m, n) = (1, 1). Power modulation of this mode is found to correlate with the power modulation of the (1,1) kink mode in the quasi-stationary intervals, and significant bicoherence was measured, both indicating non-linear interaction. The frequency ratio of the two modes was calculated with an instantaneous frequency following algorithm and was found to be in the 0.5-0.7 range. The LFSP is expected to play a role in the partial magnetic reconnection process, hence every sawtooth crash model involving such reconnection may be affected by the existence of the LFSP.

1. Introduction

The sawtooth oscillation is a periodic collapse phenomenon widely observed in tokamaks. It develops in the plasma core when the safety factor on-axis (q_0) is below 1. In the core, the temperature and density ramp up slowly – also exhibiting oscillations – over most of the sawtooth period while they rapidly crash down in the remainder.

During the crash phase there is an intensive density- and heat transport outwards. The temperature and density outside the core ramp up quickly just after the crash, and decrease gradually to their equilibrium value. This effect is most noticeable on the line integrated Soft X-Ray (SXR) measurements of the plasma core, where the repeating sequence of slow growth and sudden drop of intensity gives the characteristic sawtooth shape.

The sawtooth phenomenon is important for various reasons. The plasma can survive the performance-reducing drops of the main core plasma parameters, but the coupling of sawteeth to other, more harmful modes [1] can result in a substantial confinement degradation. Sawteeth might also pose a threat to plasma self-heating [2]. On the other hand, the sawtooth instability will remove helium ash and impurities from the core of burning plasmas, thereby preventing the degradation of the core temperature [3]. Thus the goal

is to control the sawteeth, not to totally avoid them. For these reasons, significant effort has been placed by the fusion community in observing, controlling and understanding the sawtooth instability.

Ever since the first observation, sawteeth have been connected to the $(1,1)$ internal kink mode, which is a well-known sawtooth precursor. It is characterized by an $(m,n) = (1,1)$ spatial structure, where m and n are the poloidal and toroidal mode numbers, respectively. Most of the sawtooth control methods rely on influencing the $(1,1)$ internal kink mode, that can be realized with a variety of heating and current drive techniques. The knowledge of how to control sawteeth has improved significantly in recent years [4], however, the physical processes that govern sawtooth oscillations remain only partially understood.

For example, the details of the crash mechanism itself still need to be revealed. The importance of higher order harmonics of $(1,1)$ has recently been investigated on ASDEX Upgrade [5] and HT-7 [6]. It has been proposed that the interaction of the $(1,1)$ kink and higher order harmonics can lead to a stochastization of the plasma core. These results fit well into the stochastic model [7] of the sawtooth crash. The stochastic model proposes the formation of a broad ergodic zone in the vicinity of the $q = 1$ surface that causes the collapse. The exact generation mechanism of such an ergodic zone, however, is yet unknown.

2. The low frequency sawtooth precursor (LFSP)

Careful analysis of the precursor phase on ASDEX Upgrade [8, 9] and HT-7 [10] showed, that a low frequency signal component (lower than the $(1,1)$ frequency) is visible on the central SXR signals, and it gains energy just before the sawtooth crash. Observations of a second, lower amplitude and lower frequency $n = 1$ mode have also been reported on JET [11]. This signal component is called the Low Frequency Sawtooth Precursor (LFSP). The existence of this low frequency mode and its possible interaction with the internal kink fits well into the stochastic model [8], and can be a key element in the understanding of the crash mechanism. In this paper we focus on the detailed analysis of the data from the central soft X-ray channels of ASDEX Upgrade in order to better understand the behaviour of the LFSP, and the connection between it and other sawtooth precursor modes.

Properties of this low frequency sawtooth precursor (LFSP) have been studied in detail in NBI (neutral beam injection) heated ASDEX Upgrade discharges with pronounced sawtooth activity based on soft X-ray (SXR) measurements [9]. In these discharges the enhanced toroidal rotation raises the frequency of the modes in the laboratory frame, and thus relieves the separation of the (1,1) and LFSP modes. Various shots have been selected from the shotnumber range of #20975 to #24006.

Most of the analysis tools used in this paper are based on linear continuous time-frequency transformations such as the Short Time Fourier Transformation (STFT) and the Continuous Wavelet Transformation (CWT) [12]. Continuous transformations have the advantage of being time-shift invariant that is crucial in transient signal analysis. By using linear transformations we are able to calculate the power distribution of the signal over the time-frequency plane called the spectrogram (in case of using STFT). In every investigated case the LFSP component was visible on the spectrograms already 20-40 ms before

the sawtooth crash, an example is shown in figure 1.

The LFSP was investigated during different heating- and active sawtooth control schemes (NBI, NBI+ECRH, NBI+ICRH). Investigation in the absence of NBI was not possible due to the constraint on plasma rotation explained before. The LFSP was observable in all cases with a similar time-frequency structure. The fact that the main phenomena are the same during different shots from different campaigns from year to year as well as with different heating schemes supports the generality of the observed behaviour.

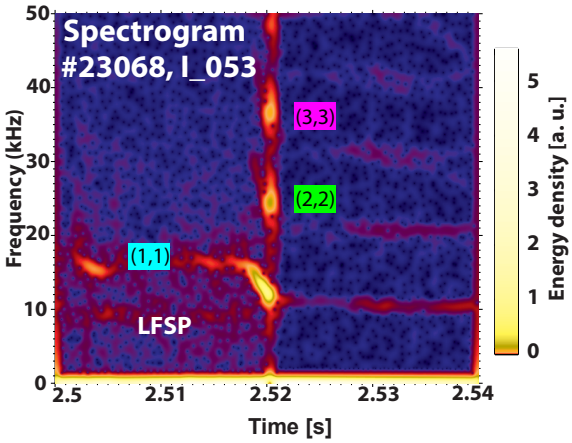

Figure 1: *The (1,1) mode and its harmonics are clearly visible before the crash. Another signal component, identified as the LFSP appears with a frequency lower than the (1,1) mode.*

We developed a new tool to estimate the frequency evolution of low energy modes such as the LFSP. We use a global ridge following algorithm based on graph theory [9]. The spectrogram is represented as a graph. Each time-frequency point is represented by a node, edges connect each node at a given time point with all the nodes in the following time point. The edges are weighted according to the amplitude of the nodes and their difference in frequency. In this representation the frequency modulation of the investigated mode is represented by the global shortest path in the graph that can be found by a modified version of Dijkstra's shortest path algorithm [13]. Figure 2 shows an example of the estimated spectrogram ridges as well as the frequency ratios of the modes as a function of time.

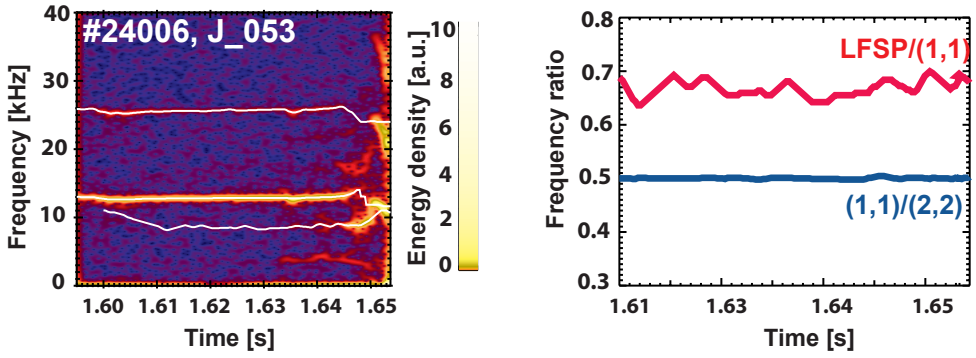

Figure 2: *Left: example spectrogram of the sawtooth crash, frequency modulation of the modes overplotted with white. Right: Frequency ratios of the different modes as a function of time.*

The frequency ratios were averaged within one shot for the several sawtooth crashes within the a selected crash group. As a benchmark of the method we checked the frequency ratio of the (1,1) and the (2,2) modes, and it was 1/2 in all cases. This result supports the reliability of the frequency following algorithm. Although there are some uncertainties, it seems to be clear that the LFSP/(1,1) ratio is not a low order rational, and it is between 0.5-0.7 in all the investigated cases.

The appearance of the low frequency component is usually visible several tens of milliseconds before the crash, but the energy of the component is very low during most of the precursor phase. The low-energy phase lasts for 10-40 ms and is followed by a swift energy gain ∼5 ms before the sawtooth crash, as observed on the spectrograms (figure 1). In order to quantitatively characterize the power evolution of the LFSP, we estimated the bandpower of the frequency range associated with it. This is done by integrating the spectrogram in frequency over a given frequency range [14]. The estimated bandpower then serves as an input for other analysis methods. We have to note that the bandpowers and the power modulation acquired with the ridge following algorithm show good agreement with each other, but the bandpower is more preferred for its simpler algorithm and also requires less computational effort.

For quantitative description of the time evolution of the energy and to estimate the growth rate of the LFSP we fitted exponential curves to the bandpowers of the LFSP for the investigated sawtooth crashes in the precursor phase. We calculated the weighted average of the fitted parameters (maximal bandpower, growth rate, background noise) in similarly behaving crash groups. The parameters show good agreement between the different shots, consequently the ramp-up of the LFSP is very uniform from the amplitude growth point of view. The average amplitude growth rate is $\gamma_A = (407\ 1/\mathrm{s} \pm 3\%)$, that suggests that the LFSP is most probably a resistive MHD mode [15]. These observations can be the basis to extract the critical values of the underlying parameters such as the LFSP amplitude necessary for the crash.

3. Interaction of the (1,1) and LFSP modes

Investigating the possible interaction of the LFSP and the (1,1) is crucial to understand the origin of the LFSP and its role in the sawtooth crash. One way to characterize the interaction of different modes is the bandpower correlation method [14] in which the bandpowers of LFSP and (1,1) are correlated with each other.

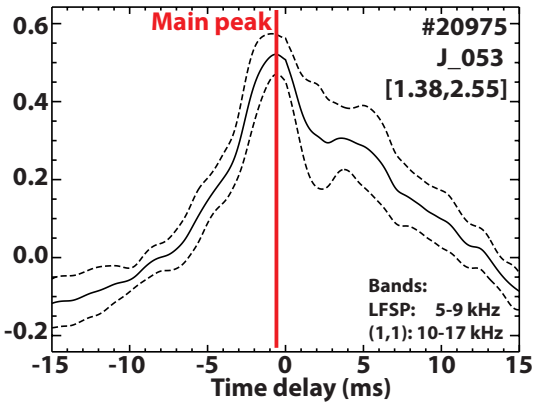

Figure 3: *Averaged bandpower cross-correlation between the LFSP and the* $(1,1)$ *mode.*

In order to improve event statistics we averaged the bandpower correlation functions for several crashes with similar behaviour. Figure 3a shows an example of the bandpower correlation functions. The 95% confidence interval (marked with two dashed lines) was calculated from the standard deviation of the averaging. We found that a $> 50\%$ correlation can systematically be shown for a wide range of shotnumbers, that implies a connection between the two modes long before the crash. Bandpower-correlation also provided a way to determine the location in which the two modes are interacting, that appears to be visible inside and also slightly outside the inversion radius [9].

The other method employed in the analysis is bicoherence, that is able to measure phase coupling between signal components [16]. Phase coupling occurs in that case, when two

frequencies and their sum frequency are present at the same time in a signal, and their phases satisfy the $\varphi_1+\varphi_2 = \varphi_3+$const. equation. The result of the bicoherence calculation is a matrix, which might be plotted as a function of two frequency variables. If the signal contains components at f_1, f_2 and $f_3 = f_1 + f_2$ frequencies, and the phases are coupled, the bicoherence take on a value close to 1 at the (f_1, f_2) point, without reference to the modes' amplitude. However, the absence of phase coupling between the components result a value near to 0. If the signal contains a harmonic and its upper harmonic at f and $2 \cdot f$ frequency, the bicoherence is close to 1 at the (f, f) point.

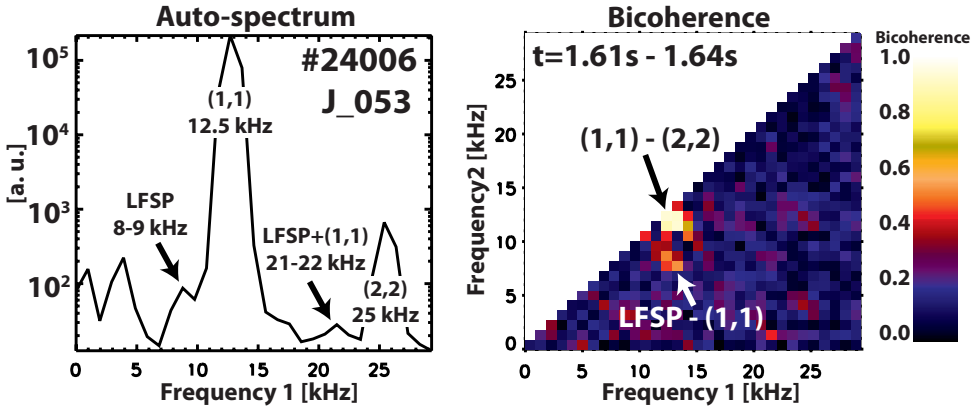

Figure 4: *Autospectrum and bicoherence calculated for the time interval t=1.61 s – 1.64 s for the crash in #24006 at 1.6537 s.*

The bicoherence plot shown on figure 4 was calculated for the time interval t=1.61 s – 1.64 s, that ends 15 ms before the crash at $t = 1.6537$ s in shot #24006. Despite the low energy of the LFSP that is barely visible on the autospectrum, we found a significant, 60% bicoherence between the (1,1) and the LFSP. This suggests the existence of a nonlinear interaction between the two modes in the early, low-energy phase of the LFSP, in agreement with the bandpower correlation analysis.

4. Spatial structure

The spatial structure of the LFSP is a key issue in understanding the phenomenon, but one has to overcome the difficulties raising in the detection and mode number estimation of a low energy, transient core mode. The only diagnostics available on ASDEX-Upgrade – at the time of investigation – that had the required spatiotemporal resolution of the plasma core are the soft X-ray cameras, for which we have applied previously developed wavelet based methods for detecting short-lived plasma eigenmodes and determining their spatial structure [9, 17]. A typical model structure for an MHD eigenmode is

$$B(\psi, \theta, \phi, t) = B(\psi) e^{i\omega t} e^{i(m\theta + n\phi)},$$

that defines the (m, n) mode numbers. Therefore, we can determine the mode number if we measure the phase of a given ω frequency mode at different spatial positions. Our mode number determination is based on the phase of the continuous analytical wavelet transform [12]. For each (u, ξ) point of the time-frequency plane, $\vartheta_{x,y}(u, \xi)$ relative phases between all (x, y) pairs of signals are calculated. For a pure harmonic structure, these relative phases would lie on a straight line as a function of the $\phi_{x,y}$ relative probe position.

The slope of the best fitting straight line gives the mode number with the residual defined as:

$$\mathcal{Q}_l(u,\xi) = \sum_{x,y} \|\vartheta_{x,y}(u,\xi) - l \cdot \phi_{x,y}\|^2_{2\pi},$$

where $l = \{m, n\}$ is the toroidal or poloidal mode number and $||\dots||_{2\pi}$ is the norm by taking the optimum shift of $\Theta_{x,y}$ by $2\pi z$, $z \in \mathbb{Z}$.

This method gives a best fitting mode number for each point on the time-frequency plane, that allows one to follow the time-frequency evolution of the mode numbers. However, mode numbers are a relevant quantity only in limited regions, where coherent modes exist. We can find these regions based on a criterion for the $\min_l\{\mathcal{Q}_l(u,\xi)\}$ values, or on wavelet minimum coherence [17], or on the combination of both, as in this paper.

With the right choice of $\phi_{x,y}$, the mode number estimation can be applied for both toroidal and poloidal mode numbers, Toroidal mode numbers were estimated using two identical SXR cameras placed 135° apart toroidally but having the same lines of sight in the poloidal cross-section. Up to 4 central channel pairs inside the sawtooth inversion radius were used for mode number estimation. For the poloidal mode numbers we had to select lines of sight in the same toroidal cross-section that are tangential to approximately the same flux surface and measure high bandpower values on the mode frequency. The mode structure distortion (caused by toroidal effects and the magnetic field gradient) can be compensated if we transform the inhomogeneous magnetic field to a homogeneous one by using a straight field line poloidal angle coordinate [18] instead of the geometrical coordinate.

According to these measurements, the mode number of the LFSP is (1,1), equal to the "classic" (1,1) kink mode, as shown in the examples in figures 5 and 6.

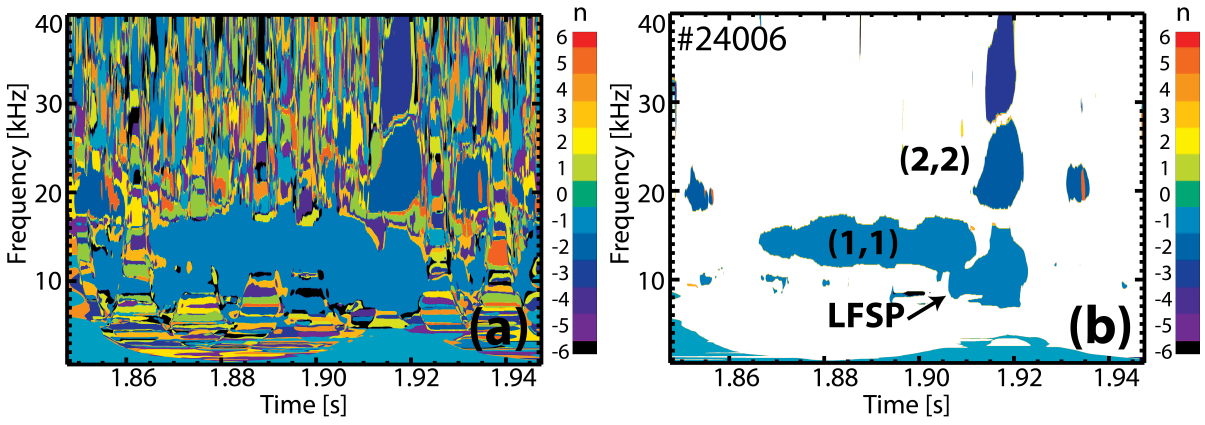

Figure 5: *(a) Toroidal mode numbers of the sawtooth precursors calculated from SXR measurements. (b) Coherence and min-$\mathcal{Q}$ filtered mode numbers. The (1,1) and harmonics are clearly observable. The toroidal mode number of the LFSP is n=1.*

5. Discussion

Our knowledge on the LFSP and its role in the sawtooth crash is not yet sufficient for a clear theoretical understanding, nonetheless, we present a few possible ways how the

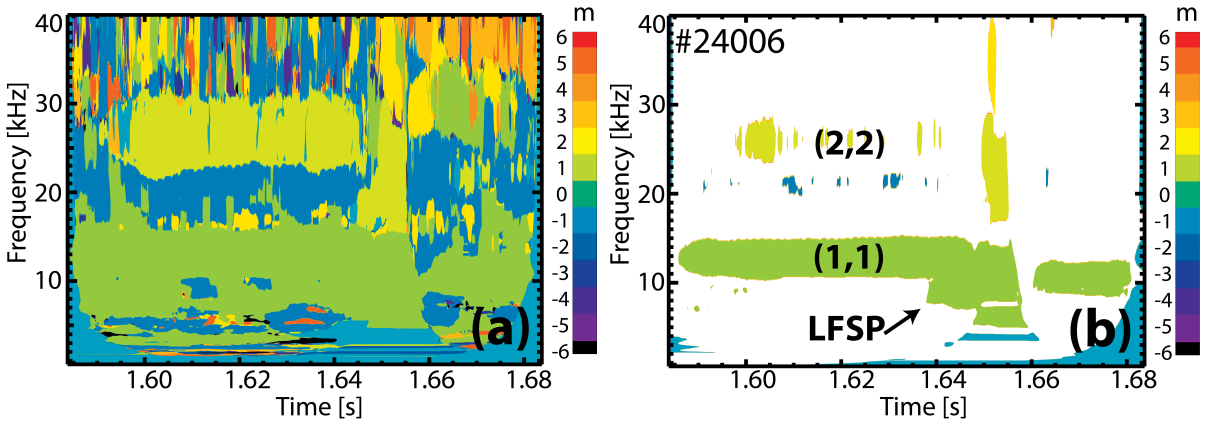

Figure 6: *(a) Poloidal mode numbers of the sawtooth precursors calculated from SXR measurements. (b) Coherence and min-$\mathcal{Q}$ filtered mode numbers. The (1,1) and harmonics are clearly observable. The poloidal mode number of the LFSP is m=1.*

LFSP can be fit into different sawtooth crash models.

If the (1,1) kink mode already exists in the plasma, it provides a strong periodic drive force that can excite other modes as well (directly via e.g. magnetic coupling; or indirectly through the change of the profiles [19]). The mode numbers of the LFSP were found to be identical to the (1,1) internal kink mode. According to the FFT amplitude and bandpower-correlation measurements, the LFSP is most probably located at the same radial position, at the $q = 1$ surface. These observations make the excitation of the LFSP by the (1,1) very likely via magnetic coupling, that is possible even if the frequency ratio is irrational [20]. A sign of this interaction is the measured bandpower crosscorrelation, and the high value of bicoherence.

It has already been shown that the (1,1) internal kink mixed with its upper harmonics can contribute to the stochastization of the plasma core [5, 21]. If we investigate the interaction of the (1,1) and the LFSP we observe that the additional small ($< 1\%$) perturbation with $f_{\mathrm{LFSP}} = 0.6 f_{(1,1)}$ mixed with the original (1,1) mode at the observed spatial position creates a relatively broad stochastic layer and an "opening" at the X point of the (1,1) island. This is shown schematically in figure 7. The important factor in this stochastization is the frequency ratio and the identical spatial structure of the two coupled modes. The fact that the two modes are interacting also outside $q = 1$ enables the formation of an ergodic layer at the outer island separatrix. Adding upper harmonics does not open up the magnetic structure as effectively as the LFSP. The generation of a broad stochastic layer near the (1,1) island separatrix and especially at the X point coincides well with the 2D electron cyclotron emission (ECE) measurements of the crash phase [6, 22, 23]. Small modifications in the perturbation amplitude can result in swift changes of the magnetic structure. It is probable that the ergodic zone visualized in figure 7 appears almost instantly when the LFSP reaches a certain critical amplitude, as was implied during the analysis of the power evolution. This could explain the sudden onset of the crash.

The implications of this model on the evolution of the q profile are consistent with the measurements, namely that the position of the $q = 1$ surface is preserved and that q on

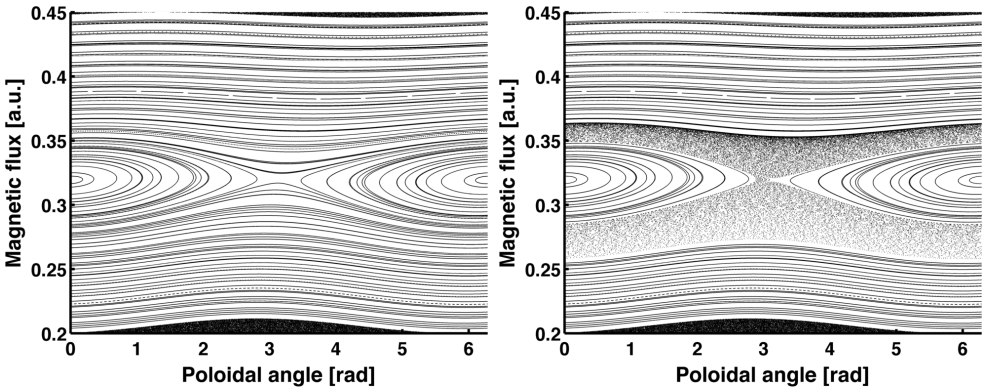

Figure 7: *(a): Sketch of the magnetic island generation as a result of the (1,1) mode. (b): X point opens up and broader stochastic region appears due to the additional presence of the LFSP.*

axis remains below unity. The interaction of the LFSP and the (1,1) kink implies a partial reconnection procedure that is consistent with the observations that heat comes out from the central core region through the X-point of the (1,1) island and the (1,1) island survives the crash [23]. The sudden onset of the crash, the rapidity of the temperature collapse and the incomplete relaxation of the current profile can also be explained by the interaction of modes with commensurate spatial structure [5].

An interesting question is why the two modes with equal spatial structure have different frequencies? One possible explanation is the difference of the mode types. According to the observed growth rate of $\gamma_A \sim 400$ 1/s, the LFSP is most probably a resistive mode [15]. On the other hand, the internal kink is often characterized as an ideal mode before the crash [24]. However, an ideal mode cannot be responsible for changes in the magnetic topology, while a resistive can be [25]. In the ASDEX Upgrade the presence of a (1,1) island is instantly visible after the crash [23]. These experimental observations cannot be described solely with ideal MHD theory.

As of today, we understand the LFSP as a secondary instability driven by the (1,1), that causes, or contributes to the crash. During the years, several different crash models have been proposed, each with experimental support [4]. The LFSP can play a role in the models that involve field line stochasticity, chaos or partial magnetic reconnection. There are indications that the sawtooth crash might be governed by different mechanisms in the various devices [26], or by a mixture of the possible mechanisms. One of the latter is the possibility that the formation of an $(1,1)$ island or an ergodic layer around $q = 1$ provides a steep temperature gradient, that excites secondary ideal MHD instabilities during the crash [19], that would explain the rapidity of the temperature and density collapse. There is also the possibility that the LFSP is excited, driven or destabilized by the changes of the parameter profiles initiated by the (1,1) mode evolution. In the latter case the interaction of the reconnection process (that is enhanced by the presence of the LFSP) and the secondary instabilities is very complex and yet unclear. These questions cannot be answered without extensive MHD simulation studies. Either way, it seems very improbable that a crash model without partial magnetic reconnection can be consistent with all the experimental observations [19, 23], and as outlined above, the LFSP can play a crucial role in the reconnection process.

Acknowledgments

This work, supported by the European Communities under the contract of Association between EURATOM and the Hungarian Academy of Sciences, was carried out within the framework of the European Fusion Development Agreement. The views and opinions expressed herein do not necessarily reflect those of the European Commission.
G. Papp is grateful for the support of the IAEA.

References

[1] O. Sauter et al. Phys. Rev. Lett., **88** (10):105001 (2002).
[2] T. Hender et al. Nuclear Fusion, **47** (6):S128 (2007).
[3] M. Nave et al. Nuclear Fusion, **43** (10):1204 (2003).
[4] I. T. Chapman. Plasma Physics and Controlled Fusion, **53** (1):013001 (2011).
[5] O. Dumbrajs et al. Nuclear Fusion, **48** (2):024011 (7pp) (2008).
[6] X. Xu et al. Plasma Physics and Controlled Fusion, **52** (1):015008 (2010).
[7] A. Lichtenberg et al. Nuclear Fusion, **32** (3):495 (1992).
[8] V. Igochine et al. Nuclear Fusion, **48** (6):062001 (5pp) (2008).
[9] G. Papp et al. Plasma Physics and Controlled Fusion, **53** (6):065007 (2011).
[10] Y. Sun et al. Plasma Physics and Controlled Fusion, **51** (6):065001 (11pp) (2009).
[11] R. Buttery et al. Nuclear Fusion, **43** (2):69 (2003).
[12] S. Mallat. *A wavelet tour of signal processing*. Academic Press, second ed. (2001).
[13] E. W. Dijkstra. Numerische Mathematik, bf1:269 (1959).
[14] G. Pokol et al. Plasma Physics and Controlled Fusion, **49** (9):1391 (2007).
[15] R. J. Hastie et al. Physics of Fluids, **30** (6):1756 (1987).
[16] Y. C. Kim et al. IEEE Transactions on Plasma Science, **7** (2):120 (1979).
[17] G. Pokol et al. AIP Conference Proceedings, **993** (1):215 (2008).
[18] M. Schittenhelm et al. Nuclear Fusion, **37** (9):1255 (1997).
[19] I. T. Chapman et al. Phys. Rev. Lett., **105** (25):255002 (2010).
[20] H. G. Schuster et al. *Deterministic chaos*. Wiley-VCH, Germany, 4th ed. (2004).
[21] V. Igochine et al. Nuclear Fusion, **47** (1):23 (2007).
[22] H. K. Park et al. Physics of Plasmas, **13** (5):055907 (2006).
[23] V. Igochine et al. Physics of Plasmas, **17** (12):122506 (2010).
[24] A. Letsch et al. Nuclear Fusion, **42** (9):1055 (2002).
[25] C. G. Gimblett et al. Plasma Physics and Controlled Fusion, **36** (9):1439 (1994).
[26] R. Hastie. Astrophysics and space science, **256** (1-2):177 (1998).